frequency offset devices. The use of self-scanning diode arrays is demonstrated here. The new technique employs a frequency tracker or counter from existing LDV systems, and a lagged correlator is used to obtain direction. The two signals I_1 and I_2 can alternately be made the complex inputs to a complex Fourier spectrum analyzer to obtain the velocity as well as direction of the scatterer.

This work was carried out when one author, Y. C. Agrawal, was supported by ONR contract N000-82-C-0019 and NOAA Sea Grant contract NA-80-AA-00077, and the other, James Riley, by a NASA student fellowship. Some numerical simulations were carried out by S. A. Little.

References

1. Y. C. Agrawal and J. R. McCullough, Appl. Opt. **20,** 1553 (1981).
2. M. J. Rudd, J. Phys. E **2,** 723 (1969).
3. Y. C. Agrawal, "A CCD Chirp-Z FFT Doppler signal processor for laser velocimetry", J. Phys. E. submitted for publication.

Reprinted from Applied Optics, Vol. *23*, page 57, January 1, 1984

Directional laser velocimetry without frequency biasing: part 2

Yogesh Agrawal and James B. Riley

In an earlier paper, Agrawal and McCullough demonstrated that a single laser beam focused at the point of measurement can be used to obtain both the magnitude and direction of local fluid velocity without the use of beam-splitting optics or frequency biasing devices. Additionally, the photoelectric signal was shown to be a zero-mean sine wave suitable for existing counter-type laser Doppler velocimeter signal processors. The method described in the above paper indicated the use of two offset photodetector arrays; the resulting photocurrents from the two arrays were correlated to give direction. In this paper we describe the implementation of the method using a self-scanning diode array. Detector sensitivity in the array is discussed and microchannel plate detectors are suggested for increased sensitivity.

I. Introduction

Agrawal and McCullough[1] demonstrated in an earlier complementary paper that a major simplification in the laser Doppler method of localized fluid velocity measurement is possible by the use of periodic detector arrays. The simplifications result in the elimination of beam-splitting optics, elimination of optical frequency shifting devices such as radial rotating gratings or acoustic Bragg cells, and optical high-pass filtering, making the signals ready for counter-type processors currently in use in conventional laser Doppler velocimeters. Essentially, a new optical and detector system was described which retains the full signal strength. The direction of motion is obtained by the algebraic sign of the integral of the product of the two photocurrents, multiplied following a 1/4-period phase shift introduced in one. In a newer development, Agrawal[3] describes the use of a charge-coupled device real-time Fourier transform analyzer to obtain both magnitude and direction of the velocity.

For the sake of completeness, reproduced here is Eq. (9) from Ref. 1, describing the incident optical field at the detector plane obtained by a cascade Fourier transform scheme[2] applicable in the Fraunhofer diffraction case:

$$E(z) = CA(l)H(z - Ml). \tag{1}$$

Here $E(z)$ is the electric field, C is a constant determining signal strength (in turn, on receiver aperture and scatterer cross section), $H(z)$ represents the Fourier transform of the receiver optics pupil function, M is magnification of the optical system, and l denotes the position of a scatterer in the laser beam at the point of measurement, i.e., $l = \bar{v} \cdot \bar{n}t$. Thus, it was shown that the optical field is a traveling wave, the direction of travel of the wave being represented by the sign of $l = \bar{v} \cdot \bar{n}t$. The detection of velocity involved the use of a periodic photodetector array, yielding a photocurrent of frequency determined by the detector array period. The determination of direction required two such periodic arrays, offset by 1/4 period, so that the two arrays yield photocurrents $\pm\pi/2$ out of phase depending on direction. If an additional $\pi/2$ phase difference is electronically introduced in one of the photocurrents and the product $\langle I_1 \cdot I_2(t - \pi/2)\rangle$ determined over each burst of signal, the sign of the product will depend on the direction of motion of the scatterer [compare Eq. (19) in Ref. 1]. Alternately, the two photocurrents are treated as the real and imaginary parts of a complex signal whose Fourier transform gives the magnitude and sign of the frequency.

In this paper a computer simulation of the signals and the use of a self-scanning linear photodiode array are described. Finally, signal processing is laid out, and the use of higher D^* (detectivity) photosensor arrays is suggested.

II. Experiment

Principally, this method calls for a much simplified optical arrangement as shown in Fig. 1, which is self-explanatory. The pinhole acts as a spatial filter, per-

---

The authors are with Woods Hole Oceanographic Institution, Woods Hole, Massachusetts 02543.
Received 23 March 1983.
0003-6935/84/010057-04$02.00/0.

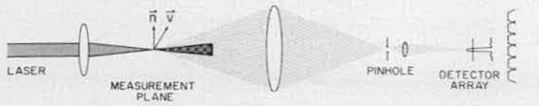

Fig. 1. Schematic of the simplified optical arrangement.

mitting only signals from a measurement volume which is well defined. The optical field at the pinhole is that described in Eq. (1). The present method of implementation calls for two periodic arrays at this position. However, since typical pinholes are of the order of 50-μm diam, whereas typical diode array spacing is 25 μm, magnification of the detector field is, in practice, necessary. In this implementation we have used one EG&G Reticon RL128G photodiode array, electronically arranged to generate two periodic responsivities as in Fig. 2.

The photocurrents $I_{1,2}$ were shown (Ref. 1) to be

$$I_i = C \int A^2(l)|H(z - Ml)|^2 \sum_n B_n \cos(nK'z + \phi_{ni})dz, \tag{2}$$

where the quantity behind the summation represents the spatially periodic detector of period $2\pi/K'$. From this it follows that the center frequency f_c in the current will be determined by the spatial period $2\pi/K'$, i.e.,

$$f_c = \frac{1}{2\pi} MuK', \text{ where } u = \bar{v} \cdot \bar{n}. \tag{3}$$

The matching of the period of the array detector and the period of $H(z)$ determines the relative response of the array. If $H(z) = \mathrm{sinc}(k\Delta z/f)$, as is the case for a rectangular aperture of width Δ [k is the wave number $2\pi/\lambda$], the requirement for matching for maximum sensitivity is that $k\Delta/(2f) = K'$, the factor 2 in the denominator appears due to the fact that the central lobe of the sinc function is 2π wide. Analogously, if $H(z) = 2J_1(kdz/f)/kdz/f)$, as is true for circular apertures of diameter d, the matching condition is similarly $kd/(2f) = 1.22\ (K')$.

Departure from these conditions will degrade the detector sensitivity and is shown in Fig. 3, where K'/K, the ratio of the width of the central lobe in $H(z)$ to the period of the array is the independent parameter. Figure 3 shows array sensitivity for both single- and dual-diode arrays. Noticeably, since neither $H(z)$ is orthogonal to the (spatially) square wave detector, the sensitivity departs from a Dirac delta function. It is of interest here to note that, if two parallel beams separated by δ are transmitted as in conventional laser Doppler velocimeters, $A(l)$ becomes periodic, representing interference fringes in the plane of measurement, i.e., $A(l) = A'(l) \cdot \cos(k\delta x/f_0)$, where f_0 is the focal length of the transmitting lens; in this case the response will appear [eq. (2)] as

$$I = A'^2(l) \int \cos^2 \left(\frac{Mk\delta z}{f_0}\right) H(z - Ml)^2 B_n \cos(nK'z + \phi_n)dz. \tag{4}$$

If now $2Mk\delta/f_0 \simeq K'$, the sensitivity functions of Fig. 3 become more sharply peaked so that such an arrangement may be employed for alignment and matching of K and K'.

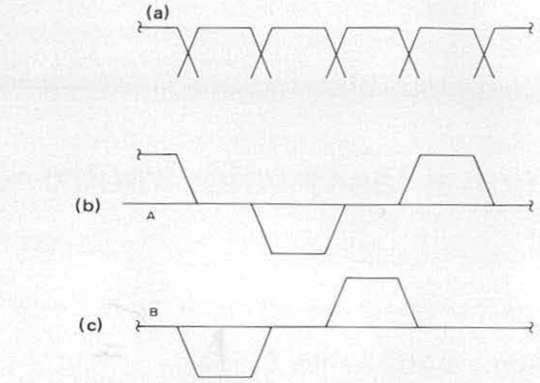

Fig. 2. Linear photodiode array, with the spatial response function as shown in (a) is electronically arranged to produce two periodic arrays (b) and (c).

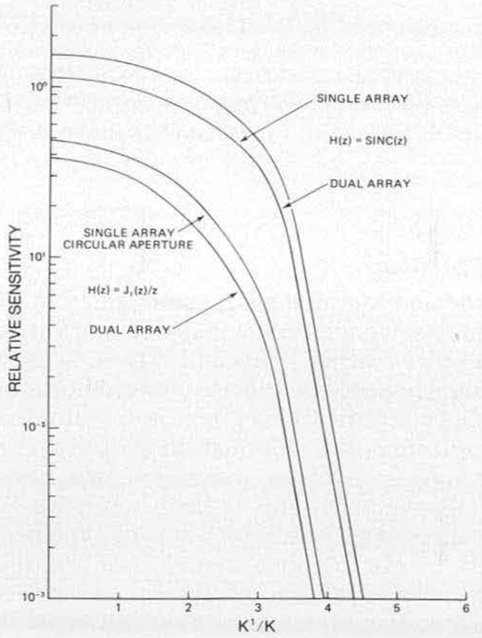

Fig. 3. Sensitivity of the array as a ratio of the width of the central lobe of the diffraction-limited image to the period of the detector array $2\pi/K'$.

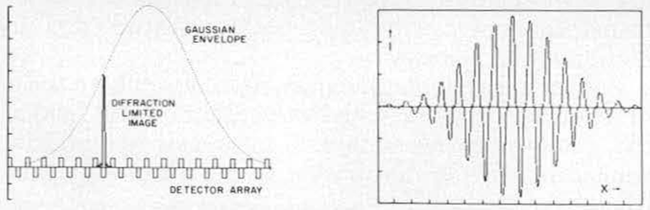

Fig. 4. Diffraction-limited image travels across the periodic response photodetector array (a) producing the photocurrent shown in (b).

In Fig. 4(a) the function $A^2(l)H^2(z - Ml)$, which represents the diffraction-limited image of the scatterer, is shown superposed on the detector responsivity. As the image traverses from left to right, a photocurrent burst as shown in Fig. 4(b) is observed. Figure 4(b) is a computer simulation, utilizing Eq. (3) with time as the abscissa.

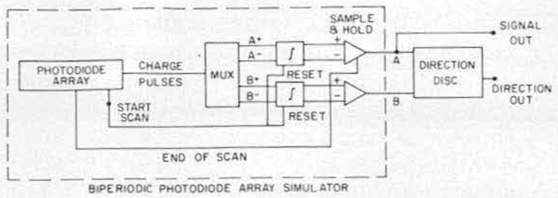

Fig. 5. Electronic block diagram.

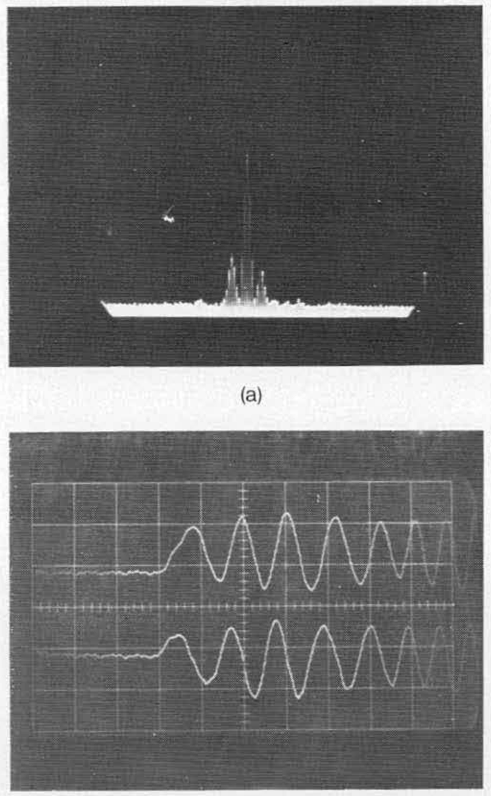

(a)

(b)

Fig. 6. Photocurrents observed when a diffraction-limited image (a) traverses across the array. In (b), the top and bottom traces represent the two photocurrents I_1 and I_2.

For the experimental implementation we chose a 1-mW He–Ne laser, a 100-mm focal length transmitting lens, a 30× (M = 30) receiving system along with an EG&G Reticon 128-element photosensor array. A microscope objective was employed behind the 100-μm pinhole to match K and K' and ensure that the scattered image traversed the full length of the detector array.

In Fig. 5 is shown a schematic of the complete electronic system. The individual diodes are clocked into a demultiplexer generating outputs A^+, A^-, B^+, and B^- of Fig. 2. The A^+,A^- and B^+,B^- channels are differentially amplified to generate charge pulses from diodes A and B. At end of scan, these values are read into a sample-and-hold circuit, the filtered output from which represents currents I_1 and I_2. One of these (say I_1) is fed into a conventional laser Doppler velocity meter frequency tracker or counter-type processor, and in another circuit the product $\langle I_1(t)I_2(t - T/4)\rangle$ is computed. Both these tasks can be combined in a single complex Fourier transform unit to be described by Agrawal.[3]

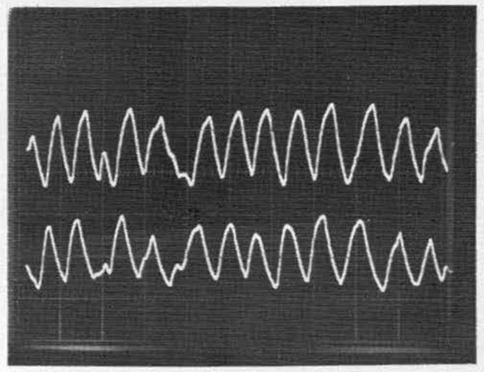

Fig. 7. Signals observed from the differential arrays A and B. The sudden change of phase in the middle of the figure is caused by the arrival of a second particle before the first leaves the probe volume.

In Fig. 6, a typical array scan of the image field generated in this manner is shown. A 2.5-μm wire was used as a scatterer in this case. Figure 6(b) shows two photocurrents A and B. The experiment was repeated to observe scattering from water. Figure 7 shows signals observed from tap water with no additional seeding; again, the two quadrature components can be observed, as also the sudden change of phase caused by arrival of a second particle into the probe volume.

Finally, the question of detector sensitivity must be addressed. The diode array employed for this experiment has a dark current of ~1 pA/diode. Thus, the dark-noise current for each detector (e.g., A^+ or A^-) consisting of thirty-two elements is 5.6 pA, which corresponds to a noise equivalent input optical power of ~5 pW. We found that the total noise (dark plus other) of the array was well below signals observed in forward scatter as in Fig. 7.

It is probably worth stressing the importance of proper optical design in this system. As is evident from Eqs. (1)–(3), the analysis is based on diffraction-limited optics. Since the aberrations of an uncorrected lens system can easily broaden $H(z)$ sufficiently to drop sensitivity in accordance with Fig. 3, the choice of suitably corrected lenses cannot be overemphasized. Yet another difficulty may arise in backscatter systems, where the typical signals will be weak, and the photodetector detectivity values could be a limiting factor. In these conditions, the low noise gain qualities of photomultipliers can be obtained in a microchannel plate detector, where the biperiodic pattern is used as the anode. In either case, specially built periodic response detectors would be required to alleviate the speed limitation imposed by scanning arrays.

III. Summary

The implementation of an imaging laser velocimeter is described. The instrument, using a new optical and detection scheme, obtains the magnitude and direction of velocity without the use of beam-splitting optics or